Surface gliding of the easy axis of a polymer-stabilized nematic liquid crystal and its dependence on the constituent monomers

Ji-Hoon Lee* and Tae-Hoon Yoon
School of Electrical Engineering, Pusan National University, Busan 609-735, Korea
(Received 7 September 2011; published 7 November 2011)

We studied the easy axis gliding of a polymer-stabilized nematic liquid crystal. The easy axis of the liquid crystal was slowly reoriented in the presence of an electric field, and the gliding process was approximated to the triple exponential functions. The different dynamics is considered to be related to the morphology of the polymers formed on the surface and in the bulk. The initial orientation of the easy axis was recovered by the elastic restoring force of the polymers after removal of the electric field. The gliding angle and reorientation time were decreased with the longer constituent monomers, and this is considered to be due to the increased anchoring and reduced surface viscosity by the increased fraction of the polymers intersticed in a liquid crystal near the surface.

DOI: 10.1103/PhysRevE.84.051701 PACS number(s): 61.30.Hn, 61.30.Pq

I. INTRODUCTION

The orientation and dynamics of a liquid crystal (LC) on the surface have been attractive research subjects over recent decades, but many unveiled issues still remain. The LC directors align along the easy axis of the surface minimizing the interaction energy [1]. With a strong (infinite) anchoring condition, the easy axis of the surface is not changed. When the surface anchoring energy is weak (finite), the easy axis can be reoriented in the presence of an external field; this phenomenon is alternatively called a *surface gliding effect* [2–5]. The previous reports about this surface gliding effect can be classified as two different mechanisms. The first case is the reorientation of the thin LC layer adsorbed on the surface; the LC layer acts as a part of the surface in this case [6–9]. The second case is the reorientation of the surface polymers; the surface polymers are dragged to a new direction by the rotation of the LC [10–13].

On the other hand, as far as we know, there has been little understanding of the surface gliding effect in the polymer-stabilized nematic LC (PSNLC). The PSNLC has drawn much attention for flexible displays owing to its greater robustness against the bending and pressing of the substrates [14,15]. In our previous work [16], we reported that the surface anchoring energy could be significantly decreased by the photopolymerized reactive-monomer (RM) layer shielding the surface potential [17,18]. Consequently, the switching voltages of the PSNLC showing 10% and 90% of transmittance (TR) could be even smaller than those of the pure LC. However, this PSNLC cell showed a severe image sticking owing to the surface gliding effect, and this should be resolved for the commercialization of flexible displays. In this paper, we study the physics of the easy axis gliding in the PSNLC system. We examined the tilt angle and time constants of LC as well as the polymers in the field-induced gliding and relaxation of the easy axis. In addition, we examined the effect of the constituent RM molecules on the surface gliding effect and found that the gliding angle and relaxation time could be reduced with the longer RM molecules.

*jihoonlee@pusan.ac.kr

II. EXPERIMENTALS

A commercial nematic LC with a negative dielectric anisotropy (ZKC7000, Chisso) was mixed with a RM mixture in a weight ratio of 8:2. The LC has the following material parameters: the relative dielectric anisotropy $\varepsilon_a = 4$, and the splay and bend elastic constants $K_{11} = 16.7$ and $K_{33} = 15.8$ pN, respectively. The RM mixture is composed of 60 wt% of 1,6-hexanedithiol (Aldrich), 30 wt% of triallyl-1,3,5-triazine-2,4,6(1h,3h,5h)-trione (Aldrich), and 10 wt% of photoinitiator (Iracure 651, Ciba Chem) [Fig. 1(a)]. A polyimide (PI) inducing a homeotropic alignment (SE5300, Nissan) was coated on an indium-tin-oxide (ITO)-deposited polycarbonate (PC) film and baked at 180 °C for 1 h. Then, the film was gently rubbed with a cotton cloth with a rubbing strength of 1.7×10^5 cm^{-1}. For the details of the definition of the rubbing strength, see Ref. [19]. After assembling the top and bottom films in an antiparallel fashion, the LC-RM mixture was injected and a UV light of 7.5 mW/cm^2 was cured for 10 min for the polymerization of the RM. The cell gap d was maintained with bead spacers with a diameter 4.0 μm, and the variance between the cells was within ± 0.1 μm. To extract the polar angle of the LC θ, we measured the phase retardation of the cell $\delta = \pi d[n_e(\theta) - n_o]/\lambda$ [Fig. 1(b)], where the wavelength of the probe beam λ was 632.8 nm and the ordinary and extraordinary refractive indices of the LC were $n_o = 1.52$ and $n_e = 1.62$, respectively. The polar angle is defined as the angle between the surface normal direction [$\vec{z}$ in Fig. 1(b)] and the principal molecular axis hereafter. Since $n_e(\theta)$ is given by $n_e(\theta) = [\cos^2\theta/{n_o}^2 + \sin^2\theta/{n_e}^2]^{-1/2}$, we can extract θ from δ [19]. The polar angle of the S-H bond of the thiol RM φ was extracted by measuring the IR absorption intensity at the wave number of 2570 cm^{-1} using a Fourier transform infrared (FTIR) spectrometer (FTS7000, Biorad). The absorption intensity A of the thiols with a polar angle of $\varphi(E)$ under an electric field E could be expressed as $A[\varphi(E)] - A[\varphi(0)] = \{A[\varphi(E_{\max})] - A[\varphi(0)]\}\sin^2[\varphi(E)]$. Thus, $\varphi(E)$ could be extracted from A with varying E. Because the thiol RM is linear shaped and the direction of the S-H bond is parallel to the molecular longitudinal direction, the polar angle of the S-H bond could be considered to be that of the thiol molecule. For the IR absorption measurement, ITO-deposited

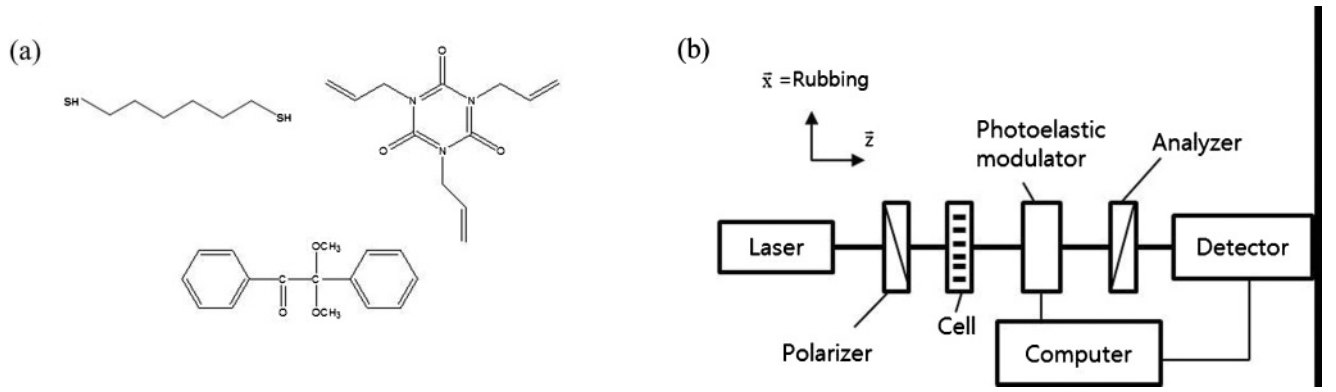

FIG. 1. (a) Chemical structures of the monomers used in the study: 1,6-hexanediol diacrylate (top left), triallyl-1,3,5-triazine-2,4,6(1h,3h,5h)-trione (top right), and photoinitiator Iracure 651 (bottom). (b) Illustration of the experimental setup to measure the optical retardation.

CaF_2 windows were used as substrates with the same surface treatment conditions. During the measurement of θ and φ, E was temporarily turned off for 5 s. This term is sufficiently longer than the time constant of the bulk LC switching with an electric field (∼20 ms) as well as shorter than the relaxation time of the easy axis (>2 min). Thus, the measured orientations of the LC and polymers give the information of the easy axis, not the instantaneously switched orientations of them by E [7]. We denoted the stabilized polar angles of the LC and thiol as θ_s and φ_s to distinguish the instantaneous field-induced angles θ_i and φ_i.

III. RESULTS AND DISCUSSION

Figure 2(a) shows the time evolution of θ_s under a bipolar voltage of 5.0 V with a frequency of 1 kHz. The threshold voltage of the cell was 3.2 V, and θ_i was about 61.5° with 5.0 V applied. The easy axis was gradually glided and saturated about 10.5°. The time evolution of θ_s was not approximated to the single exponential, but it approximated well to the triple exponential $\theta_s(t) = A_1 e^{-x/t1} + A_2 e^{-x/t2} + A_3 e^{-x/t3}$ with $A_1 = -4.43$, $A_2 = -2.14$, $A_3 = -2.91$, ${t_{1on}}^{LC} = 2.36$, ${t_{2on}}^{LC} = 12.2$, and ${t_{3on}}^{LC} = 78.7$ min. These time constants of the easy axis gliding were much longer than the instantaneous field-induced switching by an order of 10^4–10^5. Although the amplitudes A_2 and A_3 were similar, the time constant ${t_{3on}}^{LC}$ was about six times longer than ${t_{2on}}^{LC}$. We conjecture that these triple dynamics are related to the polymer morphology inside the cell. As illustrated in Fig. 2(b), three regions with different polymer morphologies could exist: near the substrate surface with polymers sticking out (zone A), bulk LCs without polymers (zone B), and around the polymers formed across the cell (zone C). The LC dynamics in these zones are expected to be different provided that the polymers give an anchoring effect to the LC.

To elucidate the relation between the LC dynamics and polymer morphology, we measured the polar angle of the thiol RM φ_s. Figure 3(a) shows the time evolution of φ_s. φ_s was gradually increased in the presence of E, i.e., the thiols were more tilted [Fig. 3(b)]. Although the error bar is not negligible, φ_s was better approximated to the double exponential functions and saturated at ∼5°, which is smaller than $\theta_s \sim 11°$. The time constants of the polymers were $t_{1on} = 23.7$ and ${t_{2on}}^{PL} = 83.7$ min, which is slower than those of the LC. These results

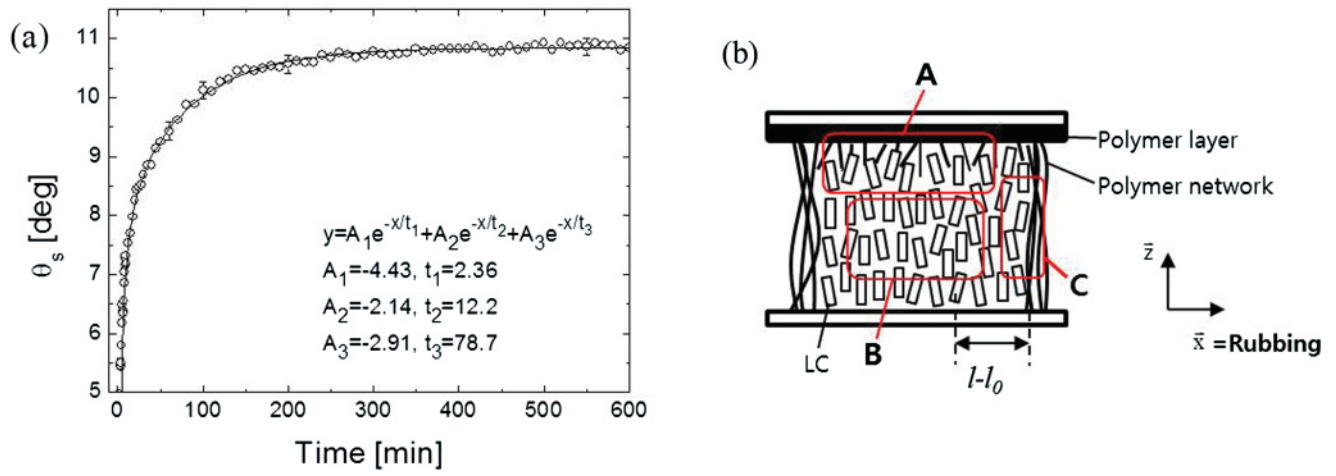

FIG. 2. (Color online) (a) Time evolution of the LC polar angle θ_s in the PSNLC cell. A bipolar voltage of 5.0 V with a frequency of 1 kHz was applied across the cell, and θ_s was measured during temporal removal of the voltage. (b) Schematic illustration inside of the PSNLC cell.

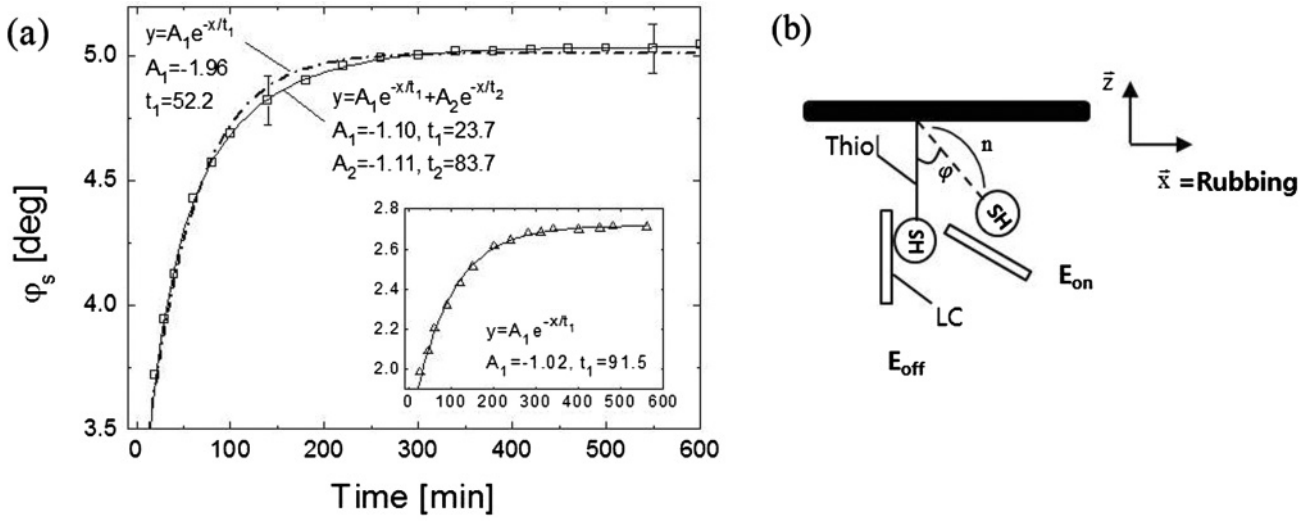

FIG. 3. (a) Time evolution of the thiol polar angle φ_s in the PSNLC cell. The inset shows the time evolution of φ_s in the RM-coated cell. A bipolar voltage of 5.0 V with a frequency of 1 kHz was applied across the cell, and φ_s was measured during temporal removal of the voltage. (b) Illustration of the rotation of LC and polymer with one side bound to the surface.

imply that the polymers are dragged by the rotating LC molecules with E. The thiols are aligned parallel to the LC directors owing to its linear shape [20]. In the presence of E, the thiols could be dragged by the LC molecules switching from the homeotropic to planar state [Fig. 3(b)]. This feature of the easy axis gliding in PSNLC implies similar physics to the results of Kurioz *et al.* [11,12] and Jánossy and Kósa [13]. Kurioz *et al.* first observed the gliding of the easy axis to the polar direction owing to the rearrangement of the polymer chains. Jánossy and Kósa reported the gliding effect in the azimuthal plane near the glass transition temperature of the surface polymer and asserted that the easy axis is created by the LC itself. Our observation also indicates that the LC rotation could define the easy axis by reorienting the polymer chains.

On the other hand, we have not yet verified the exact polymer morphologies responsible for $t_{1on}{}^{PL}$ and $t_{2on}{}^{PL}$. For this purpose, we prepared another cell whose surface was coated with RM in advance of the LC injection. The coated RM layer was photopolymerized before assembly, and then the pure LC without RM was injected. Thus, this cell has only polymers sticking out of the substrate surface and allows us to estimate the dynamics near the substrate surface [zone A in Fig. 2(b)]. The inset in Fig. 3(a) shows the time evolution of φ_s in this RM-*coated* cell. The data were approximated to a single exponential, and the time constant $t_{1on}{}^{PL,coated}$ was 91.5 min, which is comparable to $t_{2on}{}^{PL}$ [Fig. 3(a)] and $t_{3on}{}^{LC}$ [Fig. 2(a)]. Therefore, the slowest dynamics of the surface gliding is considered to be due to the anchoring of the polymers on the surface [zone A in Fig. 2(b)]. On the other hand, the time constant of the LC of the RM-coated cell $t_{1on}{}^{LC,coated}$ was 2.19 min, which is comparable to $t_{1on}{}^{LC} = 2.36$ min [Fig. 2(a)]. Thus, the fastest dynamics of θ_s ($t_{1on}{}^{LC}$) is probably for the bulk LC region [zone B in Fig. 2(b)]. In addition, the intermediate dynamics of θ_s ($t_{2on}{}^{LC}$) is considered to be due to the LC around the polymers across the cell [zone C in Fig. 2(b)].

Figures 4(a) and 4(b) show the relaxation process of θ_s and φ_s of the PSNLC cell with RM *mixed*, respectively, after removing E. The LC directors recovered the initial orientation, and the relaxation time showed a similar order to the field-induced gliding time. The polymers also recovered the initial orientation, but their relaxation times $t_{1off}{}^{PL} = 3.75$ min and $t_{2off}{}^{PL} = 58.2$ min [Fig. 4(b)] were faster than those of the field-induced gliding times $t_{1on}{}^{PL} = 23.7$ min and $t_{2on}{}^{PL} = 83.7$ min [Fig. 3(a)]. In addition, $t_{2off}{}^{PL}$ [Fig. 4(b)] was even faster than $t_{3off}{}^{LC} = 70.5$ min [Fig. 4(a)]. These results imply that the physical mechanism of the LC relaxation is related to the elastic property of the polymers. Given the thiol polymers bounded to the surface as in Fig. 3(b), dragging them with the LC rotation imposes an elastic deformation of the polymers. Upon removal of E, the distorted polymers would recover the initial orientation and give a restoring force to the LC molecules.

It also should be mentioned that the LC relaxation was a double exponential [see the nearly identical A_1 and A_2 and $t_{1off}{}^{LC}$ and $t_{2off}{}^{LC}$ in Fig. 4(a)], whereas the field-induced gliding process was a triple exponential [Fig. 2(a)]. In addition, φ_s of the polymer chains also showed a double exponential decay process [Fig. 4(b)]. Assuming the slowest relaxation process ($t_{3off}{}^{LC}$) is due to the anchoring of polymers sticking out of the surface, this result indicates a synchronized relaxation of the LC in the bulk [zone B in Fig. 2(b)] and around polymers across the cell [zone C in Fig. 2(b)]. Probably, this unusual behavior could be shown provided that the polymers across the cell form a flexible surface. Thus, these polymers might be gradually deformed by the LC directors in the field-induced gliding process, and consequently, the LC molecules in zones B and C of Fig. 2(b) might relax back in phase after the removal of E. We need to note that coarse polymer domains over micron size were not observed in the polarizing optical microscopy (POM) textures. Probably, thin polymer surfaces are dispersed in the LC substance, and this is the general feature of the thiol-ene RM growing step-polymerization process [21,22].

As mentioned in the Introduction, the surface gliding effect with a slow relaxation time fails the reliability of the display

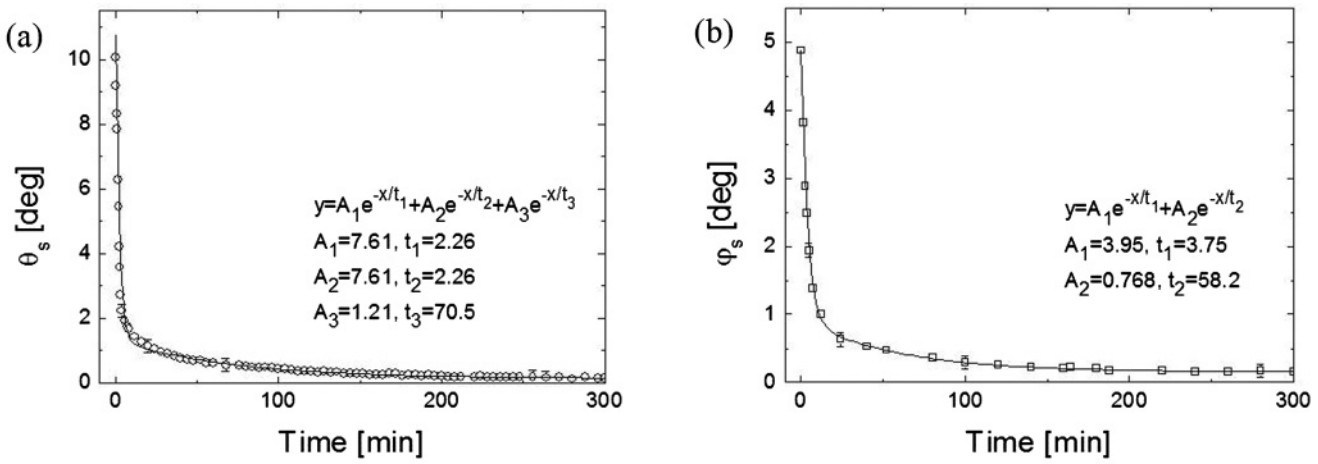

FIG. 4. Relaxation process of the (a) LC polar angle θ_s and (b) thiol polar angle φ_s of the PSNLC cell with RM mixed after removing an electric field.

devices. To resolve this problem, we varied the alkyl chain length of thiol n and examined its effect on the easy axis gliding. Figure 5(a) shows θ_s vs n after applying a bipolar voltage of 10 V with a frequency of 1 kHz for 10 h. It is apparent that the gliding angle decreases with longer n [also see Fig. 3(b)]. Figure 5(b) shows the absorption intensity of the S-H bond to the obliquely incident IR with an incident angle of 45° (A_{45°). The absorption intensity was then normalized to the absorption to the normally incident IR (A_{0°) in the zero field state. The value increases with longer n, indicating that a higher fraction of thiols align homeotropic parallel to the LC. Thus, the smaller gliding angle with a longer n is considered to be due to the increased surface anchoring by more fractions of the intersticed thiols. We also measured the time constant of the surface gliding vs n of the thiols [Fig. 6]. The gliding time of the easy axis with E [Fig. 6(a)] as well as the relaxation time after removing E [Fig. 6(b)] was shortened with longer n. We also note that the relaxation times of $t_{1\text{off}}{}^{\text{LC}}$ and $t_{2\text{off}}{}^{\text{LC}}$ depart further withshorter n [Fig. 6(b)], indicating weakened synchronized relaxation of the LC in zones B and C. Thus, the polymer morphology is highly related to the relaxation dynamics, and we are further investigating the detailed relation between them.

Let us turn to the underlying physics of the observed surface gliding effect. Because the time constant of the LC in the bulk (t_1) was faster than that near the surface (t_3), the LC molecules near the surface could be assumed to be rotated by the transmitted torque of bulk LC given by [4,7,23]

$$\Gamma_b = -(K/\xi)\sin\theta_s, \tag{1}$$

where $K = (1/2)(K_{11} + K_{33}) = 16.3$ pN is the averaged elastic constant of splay and bend deformation and $\xi = (1/E)\sqrt{K/\varepsilon_0\varepsilon_a} = 0.54$ μm is the electric field correlation length. Using the Rapini-Papoular model [24], the simultaneous restoring torque of the surface could be expressed as

$$\Gamma_s = \tfrac{1}{2}W_a \sin 2\theta_s + \tfrac{1}{2}W_b e^{-(l-l_0)/\eta}\sin 2\theta_s, \tag{2}$$

where W_a is the anchoring coefficient of the substrate surface, W_b is that of the polymers formed across the cell [zone B

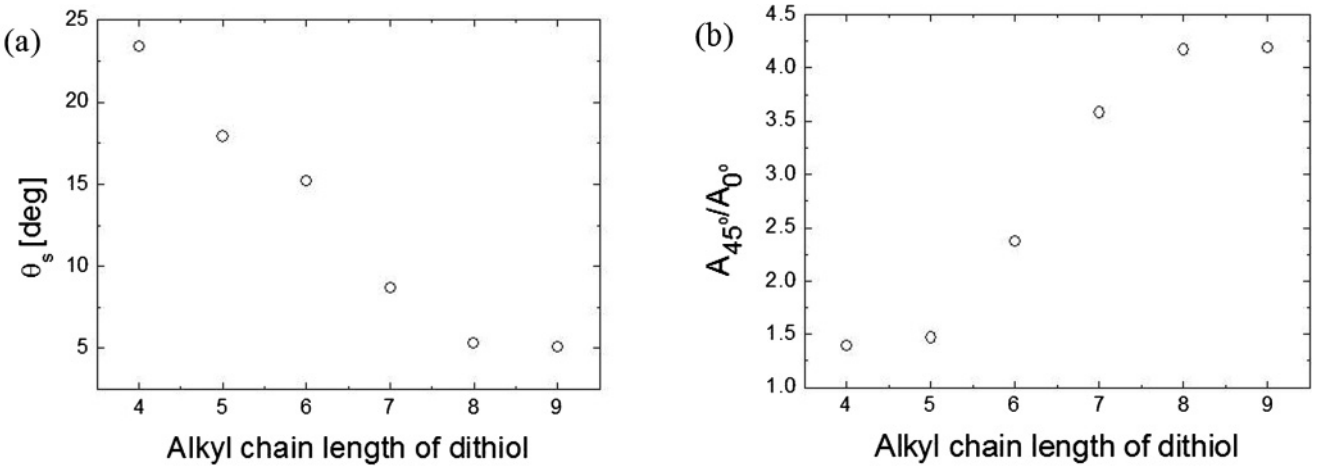

FIG. 5. (a) Gliding angle of the easy axis θ_s vs alkyl chain length n of the thiols. Bipolar voltage of 10 V with a frequency of 1 kHz was applied across the cell for 10 h. (b) Absorption intensity of the S-H bond to the obliquely incident IR with an incident angle of 45° (A_{45°) normalized to the absorption to the normally incident IR light (A_{0°).

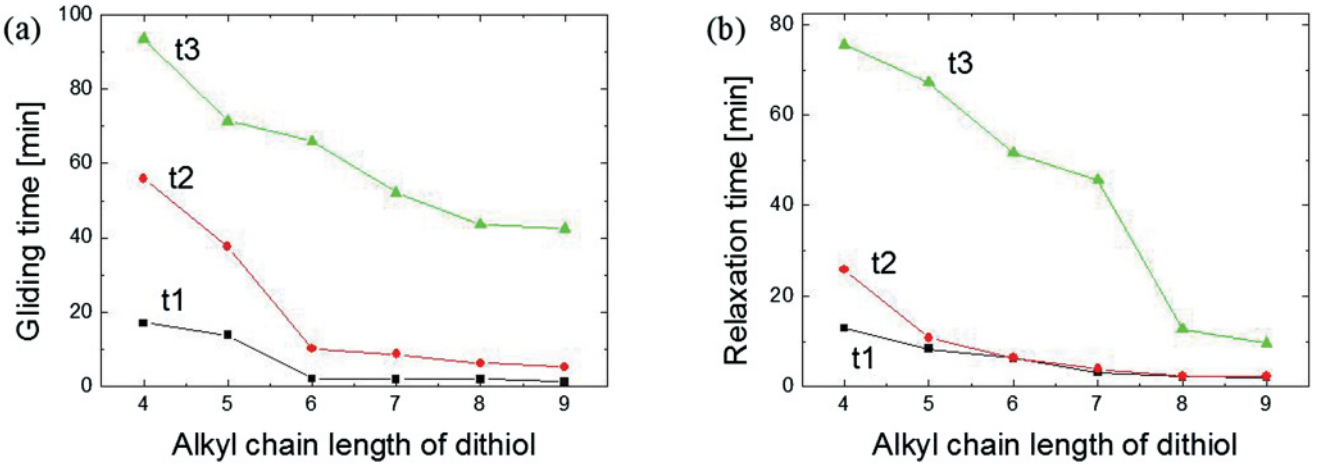

FIG. 6. (Color online) Time constant of θ_s in the (a) field-induced gliding and (b) relaxation process. t1, t2 and t3 are the time constant of the LC molecules near the substrate surface, in the bulk, and around the polymers formed across the cell, respectively.

in Fig. 2(b)], $l - l_0$ is the distance between the LC and the vertical polymer [Fig. 2(b)], and η is the associated coefficient. In addition, the LC molecules are also affected by the viscous torque given by $\gamma_s(\partial\theta_s/\partial t)$, where γ_s is the surface viscosity. Then, the torque balance equation is given by

$$(K/\xi)\sin\theta_s - \frac{1}{2}(W_a + W_b e^{-(l-l_0)/\eta})\sin 2\theta_s - \gamma_s\frac{\partial\theta_s}{\partial t} = 0. \tag{3}$$

For small θ, the solution of this equation is given by

$$\theta_s = \theta_0 e^{-t/\tau} + \text{const}, \tag{4}$$

where the time constant τ is given by

$$\tau = \frac{\gamma_s}{-K/\xi + (W_a + W_b e^{-(l-l_0)/\eta})}. \tag{5}$$

Thus, the quasiequilibrium orientation of the easy axis θ_s is determined by the torque balance equation (3), and it can be varied with E. For the cell with $n = 6$ thiol, the measured surface anchoring $W_a = 9.3 \times 10^{-6}$N/m was smaller than the field-induced transmitted torque $K/\xi = 3.0 \times 10^{-5}$ N/m, but it could not be ignored compared to K/ξ. Using this approximation, the triple dynamics of the easy axis gliding [Fig. 2(a)] could be related to the polymer morphology. For zone A near the surface [Fig. 2(b)], both W_a and W_b in Eq. (5) are non-negligible; hence a slow field-induced gliding time is expected. For zone B [Fig. 2(b)], both W_a and W_b are negligible, and a fast gliding time is expected. For zone C [Fig. 2(b)], only W_a can be ignored; hence the intermediate gliding angle could be shown.

For the effect of the length of thiols n on the surface gliding time, a larger fraction of thiols is homeotropically aligned with longer n [Fig. 5(b)], and this presumably increases W_a in Eq. (5). Thus, the field-induced gliding time constant is expected to increase. However, the time constants were decreased with longer n in both the field-induced gliding [Fig. 6(a)] and the relaxation process [Fig. 6(b)]. Therefore, the reduction of γ_s with longer n might be responsible for the decrease of the gliding and relaxation times, qualitatively. In our previous paper [17], the rotational viscosity of a polymer-stabilized chiral smectic C film was reduced with more polymer chains intersticed in the LC layer. Analogous to this, the polymer chains intersticed to the surface LC layer might reduce the surface viscosity, thus decreasing both the field-induced gliding and the relaxation time.

However, this qualitative interpretation contradicts the previous literature quantitatively. First, the estimated γ_s value from Eq. (5) using the measured gliding time t_3 of a cell with $n = 6$ thiols [Fig. 6(a)] was 2.6×10^{-6} N s/m, larger than the typical surface viscosity values with a factor of 10. In addition, as pointed out by Durand and Virga [25] and Vilfan *et al.* [26], the effective surface viscosity value was predicted to be less than the rotational viscosity γ_1, and the associated time constant was given on the order of submilliseconds. Thus, the physical meaning of the estimated γ_s value is questionable for interpreting the observed slow dynamics. Probably, a nonlinear flow effect near the surface [25] and a damping of the LC rotation owing to the intersticed polymers are related to the slow dynamics, and we have left the exact quantitative verification of them as the future work.

IV. CONCLUSION

To summarize, the easy axis gliding of the PSNLC cell showed triple dynamics, and the polymer morphology is considered to be related to the dynamics. The polymer chains were found to be reoriented with the LC rotation; thus the surface gliding effect of PSNLC originates from the reorientation of the polymers on the surface rotating with the LC molecules. The surface gliding angle and relaxation time could be reduced with longer thiol constituents that were more intersticed to the LC layer near the surface.

ACKNOWLEDGMENTS

The authors thank S.-G. Hyun (Chisso) for the liquid crystals. This work was supported by a National Research Foundation of Korea (NRF) grant funded by the Korean government (MEST, Grant No. 2011-0029198).

[1] P. G. De Gennes and J. Prost, *The Physics of Liquid Crystals* (Clarendon, Oxford, 1993).
[2] E. A. Oliveira, A. M. Figueiredo Neto, and G. Durand, Phys. Rev. A **44**, R825 (1991).
[3] P. Vetter, Y. Ohmura, and T. Uchida, Jpn. J. Appl. Phys. **32**, L1239 (1993).
[4] V. P. Vorflusev, H.-S. Kitzerow, and V.-G. Chigrinov, Appl. Phys. Lett. **70**, 3359 (1997).
[5] O. Buluy, Y. Reznikov, K. Slyusarenko, M. Nobili, and V. Reshetnyak, Opto-Electron. Rev. **14**, 293 (2006)
[6] S. Faetti, M. Nobili, and I. Raggi, Eur. Phys. J. B **11**, 445 (1999).
[7] S. Joly, K. Antonova, P. H. Martinot-Lagarde, and I. Dozov, Phys. Rev. E **70**, 050701(R) (2004).
[8] D. Fedorenko, K. Slyusarenko, E. Ouskova, V. Reshetnyak, K. R. Ha, R. Karapinar, and Y. Reznikov, Phys. Rev. E **77**, 061705 (2008).
[9] E. Ouskova, D. Fedorenko, Y. Reznikov, S. V. Shiyanovskii, L. Su, J. L. West, O. V. Kuksenok, O. Francescangeli, and F. Simoni, Phys. Rev. E **63**, 021701 (2001).
[10] D. N. Stoenescu, I. Dozov, and P. H. Martinot-Lagrade, Mol. Cryst. Liq. Cryst. Sci. Technol., Sect. A **329**, 339 (1999).
[11] Y. Kurioz, V. Reshetnyak, and Y. Reznikov, Mol. Cryst. Liq. Cryst. **375**, 535 (2002).
[12] K. Antonova, K. Slyusarenko, O. Buluy, C. Blanc, S. Joly, Y. Reznikov, and M. Nobili, Phys. Rev. E **83**, 050701 (2011).
[13] I. Jánossy and T. I. Kósa, Phys. Rev. E **70**, 052701 (2004).
[14] R. A. M. Hikmet and J. Lub, Prog. Polym. Sci. **21**, 1165 (1996).
[15] J. Lub, D. J. Broer, R. T. Wegh, E. Peeters, and B. M. I. Zande, Mol. Cryst. Liq. Cryst. **429**, 77 (2005).
[16] J.-H. Lee and T.-H. Yoon (unpublished).
[17] M. Monkade, P. H. Martinot-Lagarde, and G. Durand, Europhys. Lett. **2**, 299 (1986).
[18] V. G. Nazarenko, R. Klouda, and O. D. Lavrentovich, Phys. Rev. E, **57**, R36 (1998).
[19] G. P. Sinha, B. Wen, and C. Rosenblatt, Appl. Phys. Lett. **79**, 2543 (2001).
[20] J.-H. Lee, T.-K. Lim, Y.-W. Kwon, and J.-I. Jin, J. Appl. Phys. **97**, 084907 (2005).
[21] N. B. Cramer and C. N. Bowman, J. Polym. Sci., Part A **39**, 3311 (2001).
[22] C. E. Hoyle and C. N. Bowman, Angew. Chem., Int. Ed. **49**, 1540 (2010).
[23] J. G. Fonseca and Y. Galerne, Phys. Rev. E, **61**, 1550 (2000).
[24] A. Rapini and M. Papoular, J. Phys. Colloq. **30**, C4-54 (1969).
[25] G. E. Durand and E. G. Virga, Phys. Rev. E **59**, 4137 (1999).
[26] M. Vilfan, I. D. Olenik, A. Mertelj, and M. Čopič, Phys. Rev. E **63**, 061709 (2001).